Development 135, 2043-2053 (2008) doi:10.1242/dev.015818

Progressive myopathy and defects in the maintenance of myotendinous junctions in mice that lack talin 1 in skeletal muscle

Francesco J. Conti[1], Amanda Felder[2], Sue Monkley[3], Martin Schwander[1], Malcolm R. Wood[4], Richard Lieber[2], David Critchley[3] and Ulrich Müller[1,*]

The development and function of skeletal muscle depend on molecules that connect the muscle fiber cytoskeleton to the extracellular matrix (ECM). β1 integrins are ECM receptors in skeletal muscle, and mutations that affect the α7β1 integrin cause myopathy in humans. In mice, β1 integrins control myoblast fusion, the assembly of the muscle fiber cytoskeleton, and the maintenance of myotendinous junctions (MTJs). The effector molecules that mediate β1 integrin functions in muscle are not known. Previous studies have shown that talin 1 controls the force-dependent assembly of integrin adhesion complexes and regulates the affinity of integrins for ligands. Here we show that talin 1 is essential in skeletal muscle for the maintenance of integrin attachment sites at MTJs. Mice with a skeletal muscle-specific ablation of the talin 1 gene suffer from a progressive myopathy. Surprisingly, myoblast fusion and the assembly of integrin-containing adhesion complexes at costameres and MTJs advance normally in the mutants. However, with progressive ageing, the muscle fiber cytoskeleton detaches from MTJs. Mechanical measurements on isolated muscles show defects in the ability of talin 1-deficient muscle to generate force. Collectively, our findings show that talin 1 is essential for providing mechanical stability to integrin-dependent adhesion complexes at MTJs, which is crucial for optimal force generation by skeletal muscle.

KEY WORDS: Integrin, Talin, Muscular dystrophy, Myopathy, Mouse

INTRODUCTION

Adhesion of muscle fibers to the extracellular matrix (ECM) is essential for skeletal muscle development and integrity and is mediated by two protein complexes: the dystrophin glycoprotein complex (DGC) and complexes formed by members of the integrin superfamily. The DGC is crucial for muscle integrity as exemplified by the fact that mutations in components of the DGC cause muscular dystrophy (Davies and Nowak, 2006; Durbeej and Campbell, 2002; Durbeej et al., 1998; Straub et al., 1997). Far less is known about the function of integrins in muscle. Integrins are heterodimeric ECM receptors consisting of α- and β-subunits (Hynes, 1992). Skeletal muscle fibers in vertebrates express many integrin subunits, including the β1-subunit and its partners α1, α3, α4, α5, α6, α7 and αv (Gullberg et al., 1998). β1 integrins appear to have partially redundant functions in skeletal muscle. Accordingly, inactivation of all α/β1 integrins by CRE/lox-mediated ablation of the β1-subunit gene causes defects in myoblast fusion and sarcomere assembly that are not observed in muscle lacking individual integrin α-subunits (Schwander et al., 2003). Of all integrin α-subunit gene knockout mice, muscle defects have only been observed for mice with mutations in the integrin α5- and α7-subunit genes, and the phenotypes manifest later than in β1-deficient mice. Chimeric mice that lack the integrin α5β1 in muscle develop dystrophic symptoms (Taverna et al., 1998). Mutations in the gene for the murine integrin α7-subunit cause defects in myotendinous junctions (MTJs) (Mayer et al., 1997) and humans with mutations in the integrin α7-subunit gene suffer from myopathy (Hayashi et al., 1998).

The cytoplasmic domains of integrins bind to many cytoskeletal and signaling proteins (Geiger et al., 2001; Liu et al., 2000), raising questions about the specific contributions of individual proteins to integrin function. Talin 1 is a major integrin effector. It binds to the cytoplasmic domain of several integrin β-subunits and connects β1 integrins at focal adhesions to the actin cytoskeleton (Critchley, 2000). Talin 1 binds to focal adhesion components such as vinculin and focal adhesion kinase (FAK; Ptk2 – Mouse Genome Informatics), two important regulators of actin dynamics (Mitra et al., 2005; Ziegler et al., 2006). Importantly, the assembly of focal adhesions is dependent on mechanical force, which regulates recruitment of vinculin to focal adhesions (Balaban et al., 2001; Choquet et al., 1997; Galbraith et al., 2002; Riveline et al., 2001). Talin 1 is crucial for force-dependent vinculin recruitment, and for the strengthening of interactions between integrins and cytoskeletal proteins (Giannone et al., 2003). In addition, in vitro and in vivo studies have shown that talin 1 modulates the ligand-binding activity of the extracellular domain of integrins by a mechanism termed insight-out signaling (Calderwood, 2004a; Campbell and Ginsberg, 2004; Nieswandt et al., 2007; Petrich et al., 2007).

In skeletal muscle fibers, talin 1 is localized to costameres and MTJs (Tidball et al., 1986), and its expression is regulated by mechanical loading (Frenette and Tidball, 1998). However, the function of talin 1 in vertebrate muscle is unclear because mice with a mutation in the talin 1 (*Tln1*) gene die during gastrulation (Monkley et al., 2000). Vertebrates contain a second talin gene (*Tln2*) encoding talin 2 (McCann and Craig, 1997; McCann and Craig, 1999; Monkley et al., 2001), the function of which in skeletal muscle is likewise unknown. In vitro studies show that expression

[1]The Scripps Research Institute, Department of Cell Biology and Institute of Childhood and Neglected Disease, La Jolla, CA 92037, USA. [2]University of California and Veterans Administrative Centers, Department of Orthopaedics and Bioengineering, San Diego, CA 92037, USA. [3]University of Leicester, Department of Biochemistry, Leicester LE1 7RH, UK. [4]The Scripps Research Institute, Microscopy Core Facility, La Jolla, CA 92037, USA.

*Author for correspondence (e-mail: umueller@scripps.edu)

Accepted 31 March 2008

of talin 2 is upregulated during myoblast differentiation into myotubes, whereas talin 1 expression remains unchanged during differentiation (Senetar et al., 2007). The genomes of *C. elegans* and *D. melanogaster* contain only one talin gene, which is essential for the attachment of muscle fibers to surrounding tissue (Brown et al., 2002; Cram et al., 2003). The invertebrate ortholog of the vertebrate integrin β1-subunit gene plays a similar role, indicating that talin 1 mediates integrin functions in invertebrate muscle (Brabant et al., 1996; Brown, 1994; Brown et al., 2002; Cram et al., 2003; Gettner et al., 1995; Lee et al., 2001; Leptin et al., 1989; Volk et al., 1990). However, the mechanism by which defects in talin lead to the perturbation of adhesion sites is unclear.

To define the function of talin 1 in skeletal muscle of vertebrates, we have taken a genetic approach and crossed mice carrying a floxed *Tln1* allele with mice expressing CRE in developing skeletal muscle. We show here that talin 1 is not essential for the assembly of integrin β1-dependent adhesion complexes at costameres and MTJs. Instead, talin 1 plays an important role in stabilizing adhesion complexes at MTJs, thereby providing resistance against mechanical stress that is exerted during muscle contraction and relaxation. Surprisingly, although talin 2 is abundantly expressed in skeletal muscle, it cannot compensate for loss of talin 1, suggesting that the two talin isoforms are not entirely functionally interchangeable.

MATERIALS AND METHODS

Mouse lines and genotyping

The generation of *Tln1-flox* mice and *HSA-CRE* mice have been described (Leu et al., 2003; Nieswandt et al., 2007; Petrich et al., 2007; Schwander et al., 2003). The mice were on a mixed 129×C57Bl/6 genetic background. For genotyping, tail DNA was analyzed by PCR using primers for *Tln1* as indicated in Fig. 1: (a) 5′-AAGCAGGAACAAAAGTAGGTCTCC-3′; (b) 5′-GCATCGTCTTCACCACATTCC-3′; and (c) 5′-TAGAGAAGGTTC-AGCTGTCAGGG-3′.

Real-time PCR

Transcript levels for talin 1 and talin 2 were determined by quantitative real-time PCR (RT-PCR). RNA from gastrocnemius muscle from 5-day-old (n=3) and 6-month-old (n=3) C57Bl/6 mice was prepared using Trizol LS (Invitrogen). RNA (1.6-2 μg) was reverse-transcribed using the Superscript III System (Invitrogen). Transcripts were quantitated by RT-PCR using Chromo4 (MJ Research) and SYBR Green (Applied Biosystems). Two sets of primers were used for each transcript: Talin 1 set 1, 5′-GGAAAT-CTGCCGGAGTTTGG-3′ and 5′-TTGGCTGTTGGGGTCAGAGA-3′; Talin 1 set 2, 5′-GGGCTGGAGGGAGATGAAGA-3′ and 5′-AGA-GCCGTGCTCCACTTTCC-3′; Talin 2 set 1, 5′-AAAACCCGAATG-AGCCTGTGA-3′ and 5′-GAAATCCCTGCCATTGACTCG3′; Talin 2 set 2, 5′-GAAAACCCGAATGAGCCTGTG-3′ and 5′-GAAATCC-CTGCCATTGACTCG-3′. Primers spanned at least one exon/intron boundary and were verified in BLAST searches for specificity. To determine primer efficiency, RNA was diluted serially and linear regression analysis was applied. The slope of the resulting curve was used as a measure of PCR efficiency [$E=(10^{-1/slope})-1$]. Efficiencies of the primer pairs were 95-98%. Both set of primers produced comparable results and data from one set are shown. mRNA levels were determined using the comparative threshold (Ct) method (Livak and Schmittgen, 2001) and normalized to glyceraldehyde-3-phosphate dehydrogenase or β-actin mRNA.

Antibodies, immunohistochemistry and electron microscopy

Rabbit antibodies to talin 1 and talin 2 were produced at Animal Pharm Services (Healdsburg) using peptides corresponding to amino acids 1830-1850 (mouse talin 1) and 940-957 (mouse talin 2). Immunohistochemistry was carried out as described (Schwander et al., 2003) using the following antibodies: mouse monoclonal antibodies against vinculin (Sigma), dystrophin (clone NCL-DYS2, Novocastra), myosin heavy chain fast (Sigma) and Ilk (Li et al., 1999); rabbit polyclonal antibodies against collagen IV (Chemicon), laminin (Chemicon), talin 1, talin 2 and α7 integrin (kindly provided by U. Meyer, University of East Anglia, Norwich, UK). Electron microscopy was carried out as described (Schwander et al., 2003).

Western blotting

Gastrocnemius muscles were lysed in 1% Triton X-100 in PBS supplemented with protease inhibitor cocktail (Roche Diagnostics). Equal amounts of protein, as determined using the Micro BCA Kit (Pierce), were analyzed by western blotting with the following antibodies: talin 1, vinculin (Sigma), Erk1/2 total and phosphorylated (Cell Signaling Technology, Danvers, MA), FAK and FAK-PY397 (UBI). To verify equal loading, membranes were stripped with Stripping Solution (Chemicon) and probed with antibodies to α-tubulin (Sigma). Signal intensity was determined by densitometry using MetaMorph Optical Density analysis software (Molecular Devices). Films from three independent experiments were scanned.

Evans Blue Dye (EBD) uptake and creatine kinase assay

EBD (Sigma) was dissolved in PBS (10 mg/ml) and injected via the tail vein using 50 μl per 10 g body weight. After 5 hours, mice were sacrificed, muscles were dissected and visually inspected. Tissues were fixed overnight with 4% paraformaldehyde (PFA). Sections (12 μm) of gastrocnemius and diaphragm muscles were analyzed using an Olympus BX50WI epifluorescence microscope. Measurements of creatine kinase (CK) levels from blood samples of 6- to 7-month-old mice were performed by Antech Diagnostics (Irvine, CA). To evaluate EBD uptake after exercise, 5-month-old *Tln1HSA-CREko* and wild-type mice (4-5 per genotype) were injected with EBD solution and 1 hour later subjected to exercise. Mice were allowed to warm up by running at 10 meters/minute on a 0° incline for 5 minutes. After a 5 minute rest, mice were run at 17 meters/minute on a 0° incline for 30 minutes. Animals were returned to their cages and sacrificed 24 hours after exercise, muscles were dissected and EBD incorporation evaluated as described above.

Cardiotoxin experiments

50 μl of 10 μM cardiotoxin (Sigma-Aldrich) were injected into the calf muscles of 8- to 12-week-old mice. The controlateral leg was injected with 50 μl PBS as a control. Muscles were isolated at 5, 10 and 21 days following injection, fixed with 4% PFA and embedded in paraffin. Sections were prepared and stained with Hematoxylin and Eosin and morphology of myofibers evaluated for regeneration.

Isometric and eccentric contraction cycles

Mice were sacrificed and the fifth EDL (extensor digitorum longus) muscle was dissected in Ringer's solution (137 mM NaCl, 5 mM KCl, 1 mM NaH_2PO_4, 24 mM $NaHCO_3$, 2 mM $CaCl_2$, 1 mM $MgSO_4$, 11 mM glucose, 10 mg/l curare). Using 8-0 silk sutures, the muscle origin was secured by the tendon at a rigid post and the insertion was secured by the tendon to the arm of a dual-mode ergometer (model 300B, Aurora Scientific). Muscle was bathed in Ringer's solution, which was determined to be 10°C during measurements. Muscle length (ML) was measured, increased by 10%, and sarcomere length was measured by laser diffraction at 632.8 nm and adjusted to 3.0 μm. The EDL muscle was subjected to three passive stretches, one every 3 minutes, each time stretched 10% of ML at the velocity of 0.7 ML/second. Maximum isometric tension was measured by applying a 400 millisecond train of 0.3 millisecond pulses delivered at 100 Hz while ML was maintained constant. This measurement was repeated again after 5 minutes. The stimulation frequency chosen for these isometric contractions and the other contractions that follow was 100 Hz, as this frequency produced a fused tetanic contraction, but was low enough to prevent excessive fatigue. Each muscle underwent ten eccentric contractions (ECs), one every 3 minutes, each time stretched to 15% of ML at the velocity of 2 ML/second. Following the EC cycle, the ML was returned to its initial value and post-eccentric isometric tension was measured by applying a 400 millisecond train of 0.3 millisecond pulses, delivered at 100 Hz while ML was maintained constant. This measurement was repeated twice, at 5 minute intervals. Muscle weight was measured to determine the physiological cross-sectional area (Sam et al., 2000). Data were acquired using a CA-1000 data board and analyzed in LabVIEW 7.0 (National Instruments, Austin, TX).

All force and displacement records were stored for offline analysis. Work was calculated from the force-time and displacement-time records by creating the force-displacement relationship and integrating this relationship according to the equation:

$$W = \int_{t_1}^{t_2} F(x) \bullet dx ,$$

where t_1 represents the time at which stretch began (100 milliseconds after stimulation began), t_2 represents the time at which stretch ended (400 milliseconds after stimulation began) and x represents displacement.

RESULTS

Skeletal muscle-specific *Tln1* knockout mice

To study the function of talin 1 in skeletal muscle, we employed a conditional knockout approach using the CRE/lox system. A gene-targeting vector was generated in which exons 2-5 (of which exon 2 is the first coding exon) of the *Tln1* gene were flanked by loxP sites (Fig. 1A). A selection cassette containing a *neomycin* (*neo*) gene and a third loxP site was introduced upstream of the first loxP site. Mice were generated that transmitted the targeted allele through the germline. These mice were crossed with a CRE deleter mouse (Schwenk et al., 1995). Mice with different recombination events were recovered. In one line, only the *neo* cassette was lost, maintaining floxed exons 1-4 (referred to as conditional allele, $Tln1^{flox}$). In a second line, the floxed region including the *neo* cassette and exons 1-4 were removed (referred to as deleted allele, $Tln1^{-}$) (Fig. 1A). $Tln1^{flox/flox}$ mice showed no overt abnormality, demonstrating that the presence of loxP sites did not affect *Tln1* function (data not shown). $Tln1^{-/-}$ embryos died at gastrulation (6.5-7.5 days post-coitum) (data not shown), thus phenocopying mice in which the *Tln1* allele has been ablated (Monkley et al., 2000).

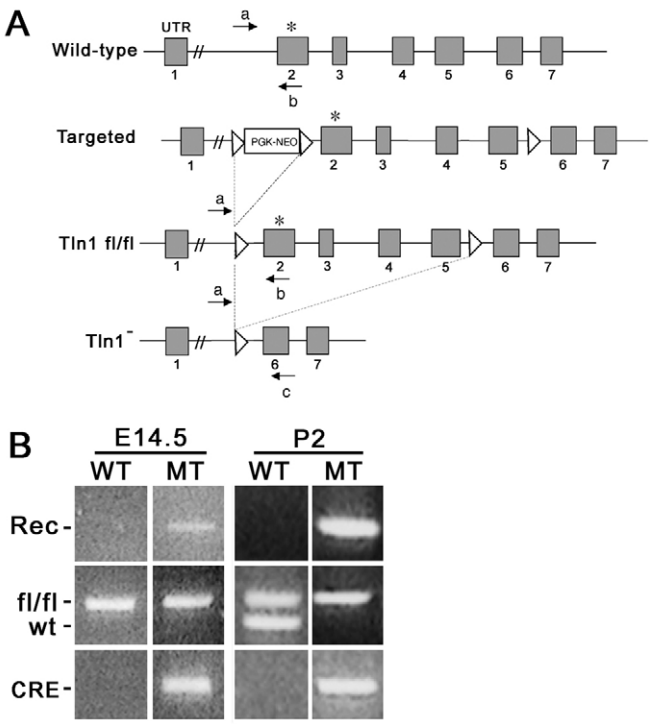

Fig. 1. Generation of the talin 1 conditional allele. (**A**) Scheme of the targeting strategy. Homologous recombination of the targeting construct into the *Tln1* gene introduced a loxP site (triangle) downstream of coding exon 5 and a floxed *pgk-neo* cassette upstream of the first coding exon (exon 2). CRE expression induced three recombination events: (1) Type II deletion: removal of the *neo* cassette (Tln1 fl/fl); (2) Type III deletion: removal of exons 1-4 (not shown); (3) Type I deletion: removal of *pgk-neo* and exons 1-4 (Tln1⁻). Primers a, b and c were used for the PCR reactions shown in B. (**B**) Recombination pattern observed by PCR on DNA extracted from E14.5 and P2 wild-type (WT) and *Tln1HSA-CREko* mutant (MT) littermates. (Top row) A 707 bp band indicative of the recombined allele (Rec) was observed in samples from *Tln1HSA-CREko* mice. (Middle row) The presence of floxed (fl) and wild-type (wt) alleles was confirmed. (Lower row) The presence of CRE recombinase was confirmed.

To abolish talin 1 expression in skeletal muscle, we took advantage of mice that express CRE under the control of the human skeletal α-actin (*HSA*; *ACTA1* – Human Gene Nomenclature Database) promoter (*HSA-CRE*) (Leu et al., 2003; Schwander et al., 2003). We have previously shown that the *HSA-CRE* transgene is expressed as early as embryonic day (E) 9.5 in somites, and throughout all muscle groups by E14.5 (Schwander et al., 2003). $Tln1^{flox/flox}$ were mated with $Tln1^{flox/+}$ mice that also contained a *HSA-CRE* transgene ($Tln1^{flox/+}$ $HSA\text{-}CRE^{+/-}$) to obtain mutant ($HSA\text{-}CRE^{+/-}$ $Tln1^{flox/flox}$, referred to as *Tln1HSA-CREko* mice) and control ($HSA\text{-}CRE^{-/-}$ $Tln^{flox/flox}$ or $HSA\text{-}CRE^{-/-}$ $Tln^{flox/+}$ referred to as wild type because their phenotype was indistinguishable from C57Bl/6 mice) offspring. To confirm recombination of the $Tln1^{flox}$ allele in *Tln1HSA-CREko* mice, we performed PCR analysis of DNA extracted from skeletal muscle of E14.5 and postnatal day (P) 2 mice; $Tln1^{flox/flox}$ and $Tln1^{flox/+}$ mice that lacked the *HSA-CRE* transgene were analyzed in parallel as controls. A 707 bp band corresponding to the recombined $Tln1^{flox}$ allele was detected in skeletal muscle of *Tln1HSA-CREko* mice as early as E14.5 (Fig. 1B), but not in non-muscle tissue (data not shown) or control mice (Fig. 1B).

Talin 1 expression is abolished in skeletal muscle

To confirm that we had inactivated *Tln1* in *Tln1HSA-CREko* mice, we raised in rabbits antibodies that are specific for talin 1 and for talin 2 (see Materials and methods) and analyzed protein expression in muscles including gastrocnemius, tibialis and diaphragm. At late embryonic and early postnatal ages when skeletal muscle fibers are actively forming, talin 1 expression was detected at the sarcolemma of wild-type mice but not in the mutants (Fig. 2A,B, arrows). Some cells in the mutants expressed talin 1 (Fig. 2A,B arrowheads), but we identified them by morphology and co-staining with antibodies to VE-cadherin (cadherin 5) as endothelial cells (Fig. 2E). Similarly, in muscle from 6-month-old mice, talin 1 expression was not detectable in muscle fibers (Fig. 2C,D) and only persisted in blood vessels (Fig. 2D, arrowhead). Western blot analysis carried out with extracts obtained from skeletal muscle of P2 and P8 *Tln1HSA-CREko* mice further confirmed that talin 1 expression was essentially abolished (Fig. 2F). Residual expression was likely to be due to talin 1 expressed in blood vessels. In addition, we detected talin 2 expression by western blot (Fig. 2F) and immunohistochemistry (Fig. 6M,N), but we failed to detect compensatory talin 2 upregulation upon removal of talin 1 (Fig. 2F, Fig. 6M,N).

The expression levels of the *Tln1* and *Tln2* transcripts in gastrocnemius muscle were also determined by real-time PCR. Expression levels for *Tln2* were 4- to 5-fold higher than for *Tln1* in both 5-day-old (*Tln1*, 1.03±0.16; *Tln2*, 4.70±0.44; P=0.004) and 6-month-old muscle (*Tln1*, 1.00±0.06; *Tln2*, 4.1±0.31; P=0.002) (Fig. 2G). This analysis corroborates earlier findings indicating that *Tln2* mRNA is the predominant isoform expressed in skeletal muscle (Monkley et al., 2001; Senetar et al., 2007).

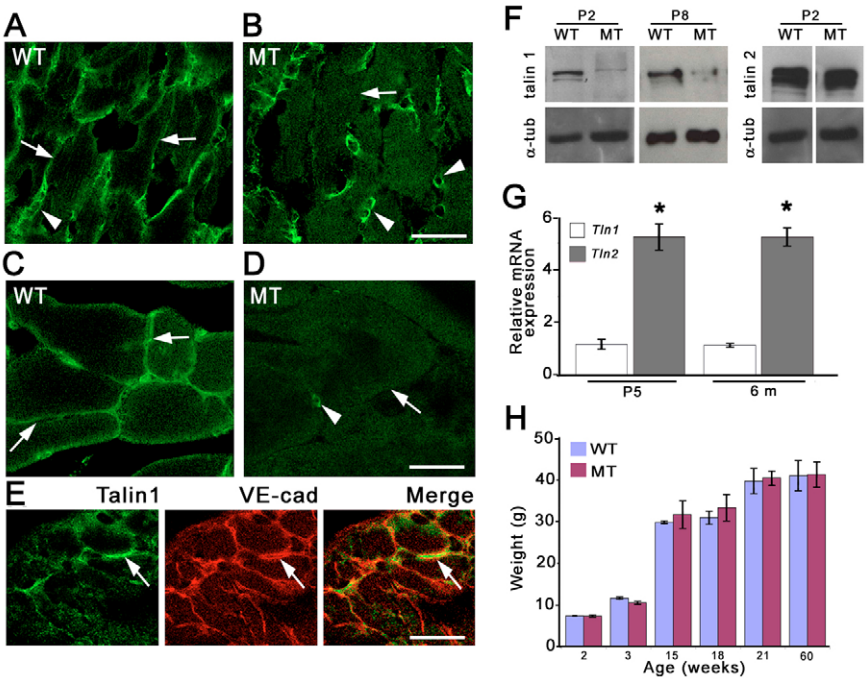

Fig. 2. Characterization of *Tln1HSA-CREko* mice. (**A-E**) Cross-sections of wild-type and *Tln1HSA-CREko* mutant muscle were stained with antibodies to talin 1 at P8 (A,B) and 6 months (C,D). Talin 1 expression was detected at the sarcolemma in wild-type (A,C) but not mutant mice (B,D). In the mutants, talin 1 expression remained in cells between skeletal muscle fibers (B,D, arrowheads) that were identified as blood vessels by staining with antibodies to VE-cadherin (E). (**F**) Western blots with extracts from P2 and P8 gastrocnemius and soleus muscle, respectively. Expression of talin 1 was markedly reduced in *Tln1HSA-CREko* mice. Residual protein levels were likely to be due to talin 1 expression in endothelial cells. Talin 2 expression was detected in muscle extracts, but no compensatory upregulation was evident. Membranes were probed for tubulin (α-tub) as a loading control. (**G**) Analysis of *Tln1* and *Tln2* transcript levels in gastrocnemius muscle by quantitative real-time PCR. Data are plotted relative to *Tln1* mRNA levels (n=3; mean ±s.e.; *P=0.004 at P5; P=0.002 at 6 months). (**H**) Growth curve of wild-type and *Tln1HSA-CREko* mice up to 60 weeks of age revealed no differences between the two genotypes. Scale bars: 25 μm in A-D; 50 μm in E.

Progressive accumulation of dysmorphic muscle fibers in *Tln1HSA-CREko* mice

Tln1HSA-CREko mice were born at the expected Mendelian ratio, were viable and fertile, were indistinguishable in appearance from wild-type littermates (data not shown), and grew at normal rates (Fig. 2H). However, histological examination revealed progressive defects in muscle fiber morphology. We analyzed several muscle groups including gastrocnemius, soleus and diaphragm collected from animals between P15 and 6 months. At P15 and P60, all muscle groups appeared normal (Fig. 3A-H; data not shown); wild-type and *Tln1*-deficient muscle fibers were regular in diameter. Morphological defects were obvious in muscle of *Tln1*-deficient mice by 6 months of age, and were more commonly observed in the diaphragm. In contrast to wild-type mice (Fig. 3I,K), muscle fibers in mutant animals appeared less regular in diameter and were enlarged (Fig. 3J,L) and distorted (Fig. 3M). Dysmorphic fibers were also evident close to the MTJs of diaphragm muscle (Fig. 3O,P). Centrally located nuclei and an accumulation of interstitial cells were occasionally detectable. However, unlike the situation in mice lacking expression of the integrin α7-subunit (Mayer et al., 1997), a diffuse centronuclear myopathy was not observed in the *Tln1*-deficient mice.

Integrins and talin 1 have been implicated in myoblast proliferation and differentiation (Senetar et al., 2007). In postnatal muscle, non-proliferating myoblasts are localized between myofibers and the basal lamina, where they constitute the satellite cell population. Upon muscle injury, satellite cells proliferate, fuse and regenerate new myofibers, which are characterized by variable size and centrally located nuclei (Shi and Garry, 2006). Immunohistochemical analysis did not provide clear evidence for talin 1 expression in satellite cells (data not shown). However, satellite cells may express low levels of talin 1 that were difficult to detect with our antibodies. Therefore, to evaluate whether the absence of a centronuclear myopathy was caused by defects in satellite cell function, we injected gastrocnemius muscles of 2-month-old mice with cardiotoxin and analyzed muscle fiber morphology 5, 10 and 21 days later. At all time points *Tln1HSA-CREko* and wild-type mice presented signs of effective muscle regeneration. Five days after toxin injection, necrotic fibers and small fibers with centrally located nuclei, indicative of regenerating fibers, were evident and immune cell infiltrate was noted (see Fig. S1A-D in the supplementary material). After 10 days, affected fibers presented with central located nuclei, but muscle architecture was largely restored (see Fig. S1E,F in the supplementary material). By 21 days, regeneration was complete (see Fig. S1G,H in the supplementary material; data not shown). We conclude that the absence of a centronuclear myopathy in *Tln1HSA-CREko* mice is not caused by an impaired capacity of mutant muscle to regenerate.

Talin 1 is not essential to maintain sarcolemmal integrity

An increase in the fragility of the sarcolemma is observed in several forms of muscular dystrophy (Carpenter and Karpati, 1979; Schmalbruch, 1975; Straub et al., 1997; Weller et al., 1990). To evaluate damage to the sarcolemma, Evans Blue Dye (EBD) was injected into 6-month-old *Tln1HSA-CREko* and wild-type mice, and muscles were dissected after 5 hours to evaluate dye incorporation. Whereas connective tissue presented a blue coloration, muscles including the diaphragm (Fig. 3Q,R), gastrocnemius and soleus (Fig. 3S,T; data not shown) failed to accumulate EBD. Occasionally, a few EBD-stained fibers were evident, independent of the genotype of the mice (Fig. 3U, arrow). Histologically, these EBD-positive fibers appeared damaged, possibly in response to normal muscle usage. This, together with the positive coloration of interstitial tissue, validated successful circulation of the dye. EBD-positive fibers in damaged muscle appeared fluorescent by light microscopy (Fig. 3X). In both wild-type and *Tln1*-deficient muscle, fluorescence was only observed in tendons and interstitial tissue, and not in muscle fibers (Fig. 3V,W).

A more sensitive indication of membrane integrity is gained by evaluating the efflux of intracellular proteins from damaged muscle fibers (Rosalki, 1989). In 6-month-old *Tln1HSA-CREko* mice,

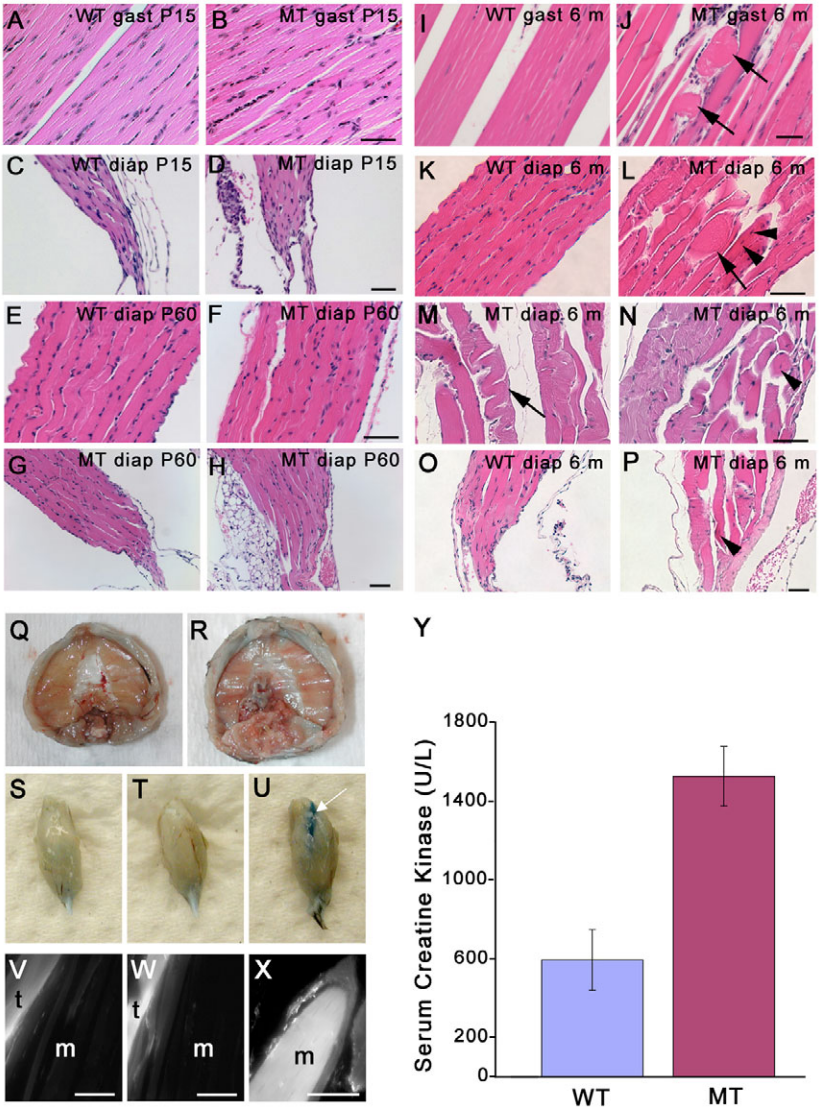

Fig. 3. Skeletal muscle defects in *Tln1HSA-CREko* mice. (**A-P**) Muscle sections from wild-type and mutant animals were stained with Hematoxylin and Eosin. Longitudinal sections from gastrocnemius (gast) and diaphragm (diap) muscles at P15 (A-D) and P60 (E-H) revealed no defects in the mutants. At 6 months, defects were observed in gastrocnemius and diaphragm muscles in mutants (J,L-N,P), but not in wild types (I,K,O). Pathological changes included enlarged (J,L, arrows) and bent (M, arrow) muscle fibers, and centrally located nuclei (L,N,P, arrowheads). Abnormal muscle fiber morphology was also evident in proximity to MTJs (compare O with P). (**Q-X**) Six-month-old mice were injected with Evans Blue Dye (EBD) and analyzed for dye uptake by bright field illumination of whole-mount tissue. Wild-type diaphragm (Q) and gastrocnemius muscle (S) did not show dye uptake, unless the muscle fibers were damaged (U) (damage was occasionally observed in wild-type and mutant mice). No dye was incorporated in mutant fibers (R,T). (V-X) Dye uptake was analyzed in sections using immunofluorescence microscopy. Tendon (t) but not muscle (m) in wild type (V) and mutants (W) had incorporated dye. In control damaged muscle from wild types (X), dye uptake was observed. (**Y**) At 6 months of age, a mild increase in serum creatine kinase levels was observed in the mutants ($n \geqslant 4$; mean ± s.e.). Scale bars: 250 μm in A-P; 200 μm in V-X.

serum creatine kinase was elevated ~3-fold compared with levels in wild-type mice (1526.20±151.44 U/l and 593.85±154.23 U/l, respectively) (Fig. 3Y). This increase is mild when compared with other mouse models of muscular dystrophy (Sonnemann et al., 2006).

Finally, we evaluated whether talin 1-deficient muscles were more susceptible to muscle fiber damage when subjected to exercise, as has been observed in other models for muscular dystrophy (Armstrong et al., 1983; Hamer et al., 2002; McNeil and Khakee, 1992; Vilquin et al., 1998). EBD was injected into 5- to 6-month-old mice and, 1 hour after injection, mice were run on a treadmill for 30 minutes. No major dye incorporation was observed in diaphragm and gastrocnemius muscle from wild-type (n=4) (see Fig. S2A,C,F in the supplementary material) or *Tln1HSA-CREko* (n=4) (see Fig. S2B,D in the supplementary material) mice. Mild EBD accumulation was only observed in one gastrocnemius muscle in one mutant mouse (see Fig. S1E in the supplementary material), and in the paraspinalis muscles of a second mouse (see Fig. S1G in the supplementary material), but the damage was mild in comparison with what has been observed in mice carrying mutations affecting DGC proteins (Sonnemann et al., 2006).

Collectively, these data suggest that sarcolemmal integrity is mildly defective when the function of talin 1 is perturbed. Mild damage to the sarcolemma was also observed in patients and mice with mutations in the gene for the integrin α7-subunit (Hayashi et al., 1998; Rooney et al., 2006).

Talin 1 is not essential for the assembly of integrin complexes at costameres

Talin binds to proteins that are localized to costameres, including β1 integrins, vinculin, actin and FAK (Critchley, 2000). Since defects in muscle fiber morphology could result from altered assembly of costameres, we assessed whether talin 1 ablation impaired costamere assembly in vivo. We analyzed the distribution of costameric proteins in 6-month-old mice by immunohistochemistry, but observed no obvious defects. β1 integrins and α-actinin were localized normally, forming a regular array (Fig. 4A-D). Talin 1 directly binds to vinculin, but vinculin was still localized to costameres in *Tln1*-deficient skeletal muscle fibers (Fig. 4E,F). Consistent with the lack of extensive sarcolemmal damage (Fig. 3), localization of dystrophin was also unaffected (Fig. 4G,H). Morphological defects of muscle fibers could be caused by defects in the basement membrane around muscle fibers, but no obvious

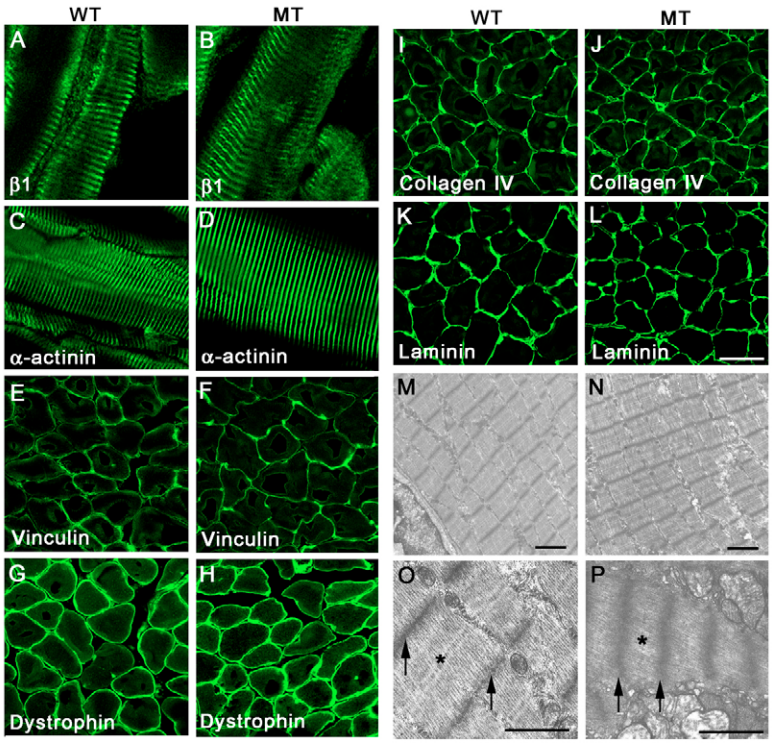

Fig. 4. Talin 1 is not essential for costamere assembly. (**A-D**) Longitudinal and (**E-L**) cross-sections of muscle from 6-month-old wild-type and *Tln1HSA-CREko* mice were stained with antibodies to costameric proteins and ECM glycoproteins and analyzed by immunofluorescence microscopy. The integrin β1-subunit, α-actinin, vinculin, dystrophin, collagen type IV and laminin were localized normally in the mutants. (**M-P**) Analysis of muscle by transmission electron microscopy. Sarcomere organization was not affected in *Tln1HSA-CREko* mice (M,N), but sarcomeres occasionally appeared hypercontracted (O,P). The Z-band was always detectable (O,P, arrows), but the A band (O,P, asterisk) was sometimes not evident in contracted muscle fibers. Scale bars: 200 μm in A-L; 2 μm in M,N; 1 μm in O,P.

defects were apparent in the localization of collagen type IV or laminin (Fig. 4I-L). Sarcomere integrity was also evaluated by electron microscopy. In both wild-type and *Tln1*-deficient skeletal muscle fibers, the sarcomeres were well organized, with Z-lines evident in both 1-month-old (Fig. 4M,N) and 6-month-old (Fig. 4O,P) mice. In *Tln1*-deficient muscle fibers, the sarcomeres occasionally appeared hypercontracted and M-bands were not always evident; the Z-line, which includes β1-integrin-containing complexes and corresponds to costameres, was always visible (Fig. 4O,P).

Talin 1 directly associates with FAK (Chen et al., 1995). Integrin binding to ECM ligands leads to activation of FAK by autophosphorylation at Tyr397, creating a binding site for Src, which phosphorylates focal adhesion components and activates MAPK signaling (Mitra et al., 2005). In *Tln1HSA-CREko* mice, expression levels and phosphorylation of FAK at Tyr397 were comparable to those of wild-type mice (Fig. 5A,D). Phosphorylation levels of Erk1/2 (Mapk3/Mapk1 – Mouse Genome Informatics) were also normal (Fig. 5B,D). Finally, western blot analysis with antibodies to vinculin and the integrin β1-subunit revealed that expression levels of these proteins were unchanged in muscle from *Tln1HSA-CREko* mice (Fig. 5C,D). Taken together, these data indicate that loss of talin 1 in skeletal muscle does not lead to major defects in the assembly of costameres, or in FAK and MAPK signaling.

Talin 1 is essential for the maintenance of the connection between integrins and myofilaments at MTJs

Alterations in muscle fiber morphology could result from defects at MTJs. Ultrastructural analysis showed that the structure of the lamina densa at MTJs, which is absent in mice with genetic ablation of β1 integrins and altered in α7 integrin mutants (Miosge et al., 1999; Schwander et al., 2003), was still visible in *Tln1HSA-CREko* mice (Fig. 6A,B). Immunostaining of sections from 6-month-old

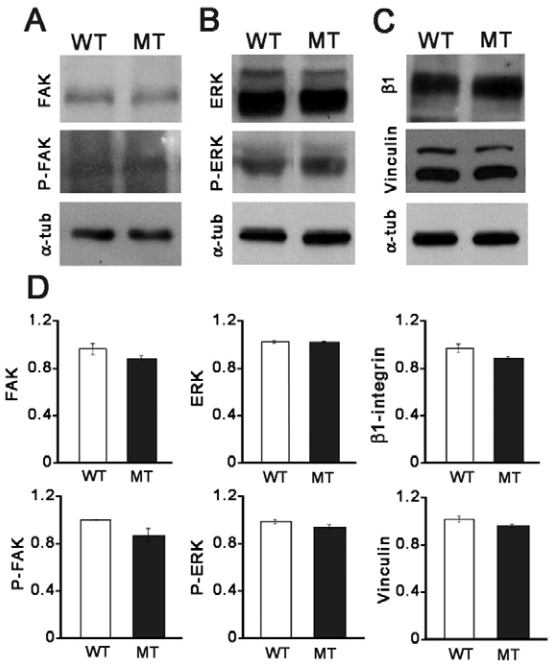

Fig. 5. Expression and phosphorylation of talin 1-associated proteins. (**A-C**) Extracts from wild-type and *Tln1* mutant gastrocnemius muscle were analyzed by western blotting. No changes were observed in levels of FAK (A), Erk1/2 (B, ERK), β1 integrin and vinculin (C). Phosphorylation of FAK at Tyr397 (A, P-FAK) and of Erk1/2 (B, P-ERK) were unaffected. Membranes were probed with α-tubulin antibodies as a loading control. (**D**) Protein expression was quantified by densitometry ($n \geqslant 3$; relative expression levels ±s.e.). No statistically significant difference was observed in expression (*P*-values: β1 integrin, 0.238; vinculin, 0.146; FAK, 0.223; P-FAK, 0.153; ERK, 0.892; P-ERK, 0.165).

mice demonstrated that the distribution of collagen IV and laminin was normal at MTJs in *Tln1* mutant animals (Fig. 6C-F). In addition, α7 integrin, vinculin and integrin-linked kinase (Ilk) localized at the MTJ, suggesting that the integrin complexes at MTJs assemble in the absence of talin 1 and are largely functional to mediate adhesive interactions (Fig. 6G-L). We also observed that talin 2 is localized at the MTJs without any obvious upregulation in the mutants (Fig. 6M,N). Taken together, these data provide strong evidence that integrin-dependent adhesion complexes still form at MTJs in the absence of talin 1.

Further ultrastructural analysis of skeletal muscle in 1- and 6-month-old animals revealed that the attachment of myofilaments at MTJ progressively failed in *Tln1HSA-CREko* mice. At the MTJs of wild-type mice, the sarcolemma was extensively folded (Fig. 7A,D). Myofilaments displayed a regular sarcomeric structure and were connected to the subsarcolemmal electron-dense plaque at the basement membrane (Fig. 7A,D,F; arrowheads). In *Tln1HSA-CREko* mice, myofilaments failed to connect to the basement membrane and were retracted (Fig. 7C,E,G). Necrotic material accumulated between the myofilaments and the basement membrane (Fig. 7C,E,G, asterisks) and included vacuoles and membranous debris. The subsarcolemmal plaque was present in *Tln1HSA-CREko* mice, but its thickness was reduced and, in particular, it was discontinuous in areas were myofilaments failed to attach (arrows in Fig. 7G). The interdigitations of muscle fibers with the tendon were also perturbed (Fig. 7C,E,G). Defects were noted in different muscles, including tibialis (Fig. 7A-C), diaphragm (Fig. 7D-G) and gastrocnemius (not shown). Ultrastructural analysis of extrajunctional areas revealed additional abnormalities that are commonly observed in dystrophic muscles, including the presence of structures that resembled vacuoles (Fig. 7E,G,I,J), suggesting some degree of degeneration. Upon closer inspection, some vacuoles could be identified as morphologically abnormal mitochondria (data not shown). These were unlikely to be artefacts of sample preparation, as normal and abnormal mitochondria were found closely juxtaposed to each other (white arrows in Fig. 7I). In some areas, excessive accumulation of mitochondria was noted (Fig. 7K,L).

Collectively, our findings show that in the absence of talin 1, integrin adhesion complexes still form at MTJs and connect to the muscle fiber cytoskeleton. However, with progressive age, myofilaments detach, suggesting that talin 1 is required for maintaining their interaction with integrin adhesion complexes during mechanical strain.

Altered mechanical properties of skeletal muscle fibers in *Tln1HSA-CREko* mice

Defects in MTJs are likely to affect the ability of skeletal muscle fibers to generate force and to resist mechanical damage during contraction. To test this hypothesis, we applied defined length changes to muscles using an ex vivo experimental setup. The fifth toe extensor digitorum longus (EDL) muscle was isolated from 2- to 3-month-old and 6- to 7-month-old mice and subjected to cyclic isometric or eccentric contractions. Isometric contractions are performed by stimulating muscle fibers to contract while keeping the length of the muscle constant, and provide a measure of the force the muscle is able to exert (Fig. 8B). Eccentric contractions are performed by lengthening the muscle while at the same time stimulating contraction (Fig. 8C) and induce damage in muscle fibers (Armstrong et al., 1983; Lieber et al., 1991). The difference in isometric stress produced by muscle fibers before and after the eccentric contraction cycle provides a measure of susceptibility to mechanical damage (Sam et al., 2000). No significant difference was observed in the length and mass of isolated wild-type and *Tln1*-deficient muscles (Fig. 8A), and all force values were normalized against the physiological cross-sectional area (Fig. 8A), which takes into account differences in muscle mass, length and in the orientation of muscle fibers (see Materials and methods). At 2 to 3 months of age, the isometric stresses produced by *Tln1*-deficient muscle fibers were comparable to those of wild-type muscle fibers

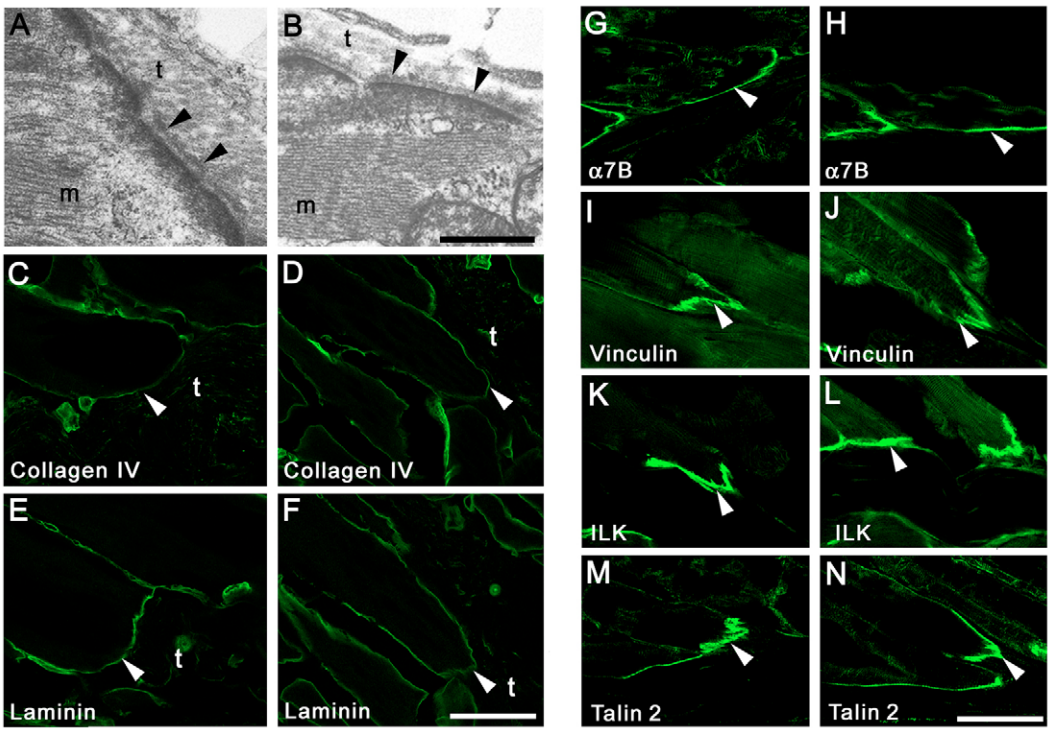

Fig. 6. Integrin complexes are maintained at the MTJ. (**A**,**B**) MTJs in diaphragm muscle from wild-type and *Tln1* mutant mice were analyzed by transmission electron microscopy to reveal the lamina densa. A continuous basement membrane (arrowheads) was present at the MTJ in mutants. (**C-N**) Localization of collagen IV, laminin, integrin α7β, vinculin, Ilk and talin 2 at MTJs (arrowheads) was analyzed by immunofluorescence microscopy. All analyzed proteins were present at MTJs in wild-type and mutant animals. t, tendon, m, muscle. Scale bars: 500 nm in A,B; 100 μm in C-F; 200 μm in G-N.

(P=0.413 pre-eccentric, P=0.892 post-eccentric) (Fig. 8D). By contrast, force production was markedly impaired in muscle obtained from 6- to 7-month-old *Tln1HSA-CREko* mice (Fig. 8E). In an eccentric contraction cycle, mutant mice showed a significant reduction in maximum pre-eccentric (P=0.0276) and post-eccentric (P=0.0358) isometric stress (Fig. 8F,G). Additionally, for older *Tln1*-deficient muscles, the peak stresses exerted during the eccentric contraction were significantly reduced from wild-type values in every eccentric contraction except the initial one, which showed greater variability (see Fig. S3B in the supplementary material). Similarly, the work performed on the muscle normalized by muscle mass was decreased in the 6- to 7-month-old *Tln1HSA-CREko* mice for each eccentric contraction when compared with the wild type (see Fig. S3D in the supplementary material). Values of peak stress

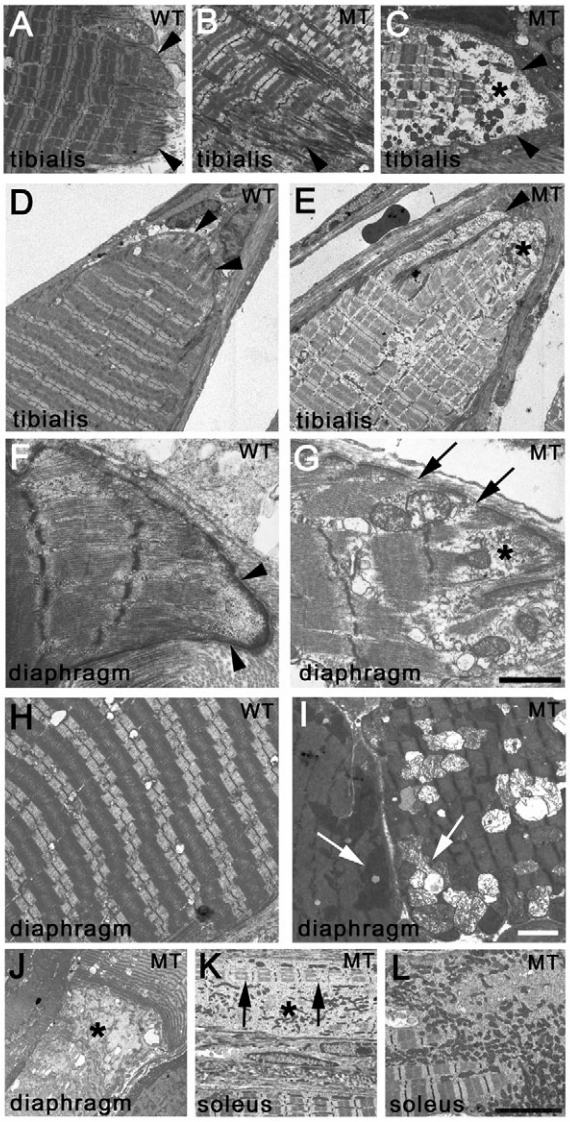

Fig. 7. Detachment of myofilaments at the MTJ. Electron micrographs of tibialis (**A-E**), diaphragm (**F-J**) and soleus (**K**,**L**) muscles collected from 1-month-old (A-C,H,I) and 6-month-old (D-G,J-L) wild-type (WT) and *Tln1* mutant (MT) mice. In wild-type mice, myofilaments connected to junctional electron-dense plaques are visible (arrowheads in A,D,F). In 1-month-old *Tln1HSA-CREko* mice, most MTJs were intact (B), but detachment of myofibers from MTJs was occasionally observed (C). In 6-month-old mutant animals, detachment of the myofibers was observed very frequently (E). Necrotic material was present where myofibers detached (asterisks in C,E,G). The thickness of the junctional plaque was reduced, and gaps were present where myofilaments failed to attach (arrows in G). Degeneration (I) and accumulation (K,L) of mitochondria were observed. Necrotic areas were observed in mutant fibers (J,K, asterisk) next to abnormal myofilaments (K, arrows). Scale bars: 3 μm in A-E,H,I; 1 μm in F,G; 10 μm in J-L.

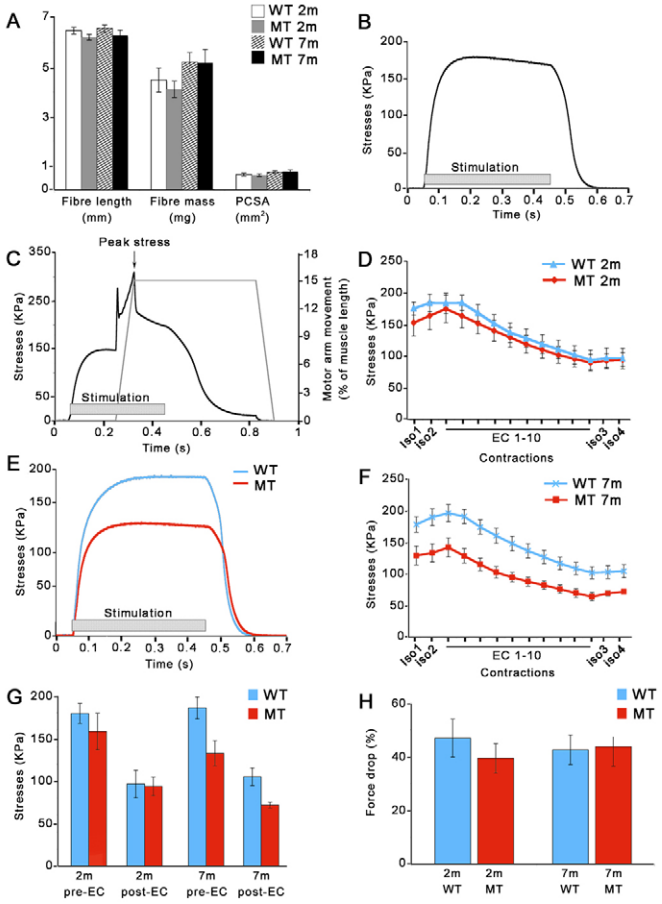

Fig. 8. Impaired force generation by Tln1-deficient muscles. (**A**) The length, mass and physiological cross-sectional area (PCSA) are similar in the fifth EDL muscle from wild-type and *Tln1HSA-CREko* mice. (**B**,**C**) Sample curves representing a single isometric and eccentric contraction, respectively. (**D-H**) Isometric and eccentric contractile properties of the fifth EDL muscle isolated from 2- and 7-month-old mice. (D) No significant difference was observed in stress exerted by 2-month-old muscles from wild-type and *Tln1HSA-CREko* mice in the eccentric contraction protocol. (E) Example of force profile of the first isometric contraction in 7-month-old mice. *Tln1*-deficient muscles exert reduced isometric stress. (F,G) In an eccentric contraction protocol, muscles from 7-month-old *Tln1HSA-CREko* mice showed a significant reduction in peak stress exerted in the pre-eccentric (P=0.0276) and post-eccentric (P=0.0358) isometric contractions as compared with wild-type controls ($n \geqslant 4$ per genotype per time point). (H) Even though *Tln1*-deficient muscles generated less force than controls, the force drop was comparable between genotypes, suggesting enhanced susceptibility to damage in the mutants. All force values were normalized against the PCSA of the muscle (mean ±s.e.).

and work were not significantly different between the muscles obtained from 2-month-old wild-type and mutant mice (see Fig. S3A,C in the supplementary material). The forces generated by wild-type and mutant fibers decreased during the eccentric contraction protocol (Fig. 8D,F). At both 2 and 7 months, the force drop was comparable between wild-type and *Tln1*-deficient muscles (Fig. 8H). However, because 7-month-old mutant muscles exerted considerably less force during the contraction protocol, reduced damage and fatigue and consequently a smaller force drop were expected. The greater than expected force drop in mutant muscle suggests that *Tln1*-deficient muscle was susceptible to eccentric-contraction-induced damage. These data are consistent with a failure in the attachment of skeletal muscle fibers at MTJs. Overall, we conclude that ablation of talin 1 causes a progressive impairment of the capacity of muscle to generate and to bear force.

DISCUSSION

We show here that talin 1 is crucial for the maintenance of integrin attachment sites at MTJs. *Tln1HSA-CREko* mice were viable and fertile, but suffered from a progressive myopathy. Whereas integrins and some of their effectors such as FAK, Ilk and vinculin still were localized to muscle attachment sites at costameres and MTJs, MTJs showed structural abnormalities. Defects in the ultrastructure of MTJs, such as decreased interdigitations of muscle and tendon and retraction of myofilaments from electron-dense plaques at the plasma membrane, indicate that in the absence of talin 1 the mechanical connection of actin filaments and integrins at the MTJ was compromised. By contrast, sarcolemmal integrity was largely maintained. Defects in skeletal muscle were prominent in 6- to 7-month-old mice, and were only occasionally noted in 1- to 2-month-old animals, suggesting that the defects were caused by mechanical failure of MTJs under duress. In agreement with this finding, isolated muscle fibers from 7 months but not 2 months were severely compromised in their ability to generate force.

Previous studies have shown that in invertebrates, talin is essential to mediate interactions between integrins and the muscle fiber cytoskeleton (Brown et al., 2002; Cram et al., 2003), but the mechanism of talin function has remained unclear. By taking advantage of a vertebrate model system that provides greater access to study the biophysical properties of muscle, we now provide evidence that talin 1 has an important biomechanical role in muscle. Studies with cells in culture have shown that talin 1 localizes to focal adhesions, where it interacts with β1 integrins, FAK, vinculin and actin (Borowsky and Hynes, 1998; Critchley, 2000), and with layilin in membrane ruffles (Borowsky and Hynes, 1998). The assembly of adhesion complexes at focal adhesions is controlled by mechanical force. Forces that are applied to nascent integrin adhesion sites induce a strengthening of the integrin-cytoskeleton interaction, initiating focal adhesion formation and promoting maturation (Balaban et al., 2001; Choquet et al., 1997; Galbraith et al., 2002; Riveline et al., 2001). Mechanical force accelerates the localization of vinculin to focal adhesions, which depends on talin 1 (Giannone et al., 2003). Our findings now show an important mechanical function for talin 1 in vertebrate skeletal muscle in vivo. At MTJs, integrin adhesion complexes containing the integrin α7- and β1-subunits, Ilk and vinculin assembled in the absence of talin 1. However, talin 1-deficient MTJs showed greater susceptibility to mechanical stress-induced damage. MTJs in muscle such as diaphragm that is under constant workload showed the most prominent defects. Mechanical measurements on isolated muscle fibers demonstrated that talin 1-deficient fibers generated less force than wild-type muscle fibers. MTJs in *Tln1HSA-CREko* mice still contained talin 2 but were unstable, suggesting that talin 1 and talin 2 are not entirely functionally interchangeable.

Previous studies have shown that talin 1 is of central importance for integrin function, regulating interactions of the β1 integrin with the cytoskeleton and with ECM ligands (Calderwood, 2004b; Campbell and Ginsberg, 2004; Ginsberg et al., 2005; Nieswandt et al., 2007; Petrich et al., 2007). Ablation of the gene encoding the integrin β1-subunit during skeletal muscle development leads to defects in myoblast fusion and sarcomere assembly (Schwander et al., 2003). We were surprised that we did not observe similar defects in *Tln1HSA-CREko* mice. The migration and fusion of myoblasts was not obviously perturbed, and immunohistochemical and ultrastructural analysis revealed no defects in the assembly of costameres and integrin complexes. How can these findings be reconciled? Talin 1 might still have essential functions early in skeletal muscle development, for example in myoblast migration, that have escaped detection because gene inactivation using HSA-CRE might have been incomplete at early ages. Furthermore, talin 2 may compensate for some talin 1 functions. In agreement with previous findings (Monkley et al., 2001; Senetar and McCann, 2005; Senetar et al., 2007), we observed prominent talin 2 expression in skeletal muscle. However, our findings as well as previous studies suggest that talin 2 and talin 1 are not entirely interchangeable. First, genes for talin 1 and talin 2 have been identified in all available vertebrate genomes, indicating that evolutionary pressure has maintained two talin genes. Second, *Tln1*-null mice are embryonically lethal (Monkley et al., 2000) indicating that *Tln2* cannot compensate for *Tln1* in early mouse development. Third, although talin 1 and 2 share a high degree of identity, amino acid differences in functionally important domains such as FERM and I/LWEQ (actin-binding) domains have been maintained throughout evolution (Senetar and McCann, 2005). These differences might confer specific functions to each protein. Consistent with this interpretation, talin 1 and 2 have different affinities for F-actin (Senetar et al., 2004). Fourth, talin 1 and talin 2 have distinct binding partners in skeletal muscle (Senetar and McCann, 2005). Finally, the two-piconewton slip bond between fibronectin and the cytoskeleton depends on talin 1. Talin 2 cannot compensate for the function of talin 1 in this process (Jiang et al., 2003). The latter finding suggests that talin 1 has a specialized function in force coupling, which could be especially important in maintaining MTJs under mechanical duress. Talin 2 is likely to be sufficient for the assembly of integrin adhesion complexes at MTJs, but in the absence of talin 1, MTJs progressively fail.

Our data suggest that the functions of talin 1 in the regulation of integrin activation might be tissue-specific. Unlike the situation in megakaryocytes and platelets, in which a rapid and discrete modulation of integrin affinity for the ECM is required for proper function (Calderwood, 2004a; Campbell and Ginsberg, 2004; Nieswandt et al., 2007; Petrich et al., 2007), affinity modulation may be less crucial at more stable adhesion complexes at MTJs. Importantly, integrin activation by talin was evaluated only for the integrin β1A splice variant, whereas adult skeletal muscle expresses integrin β1D, which provides a stronger mechanical link to the actin cytoskeleton.

Finally, our findings have implications for understanding disease mechanisms. Mutations that affect talin 1 and integrin α7β1 cause fragility of MTJs, but membrane damage is mild (Hayashi et al., 1998; Mayer et al., 1997). By contrast, MTJs are maintained when the DGC is affected, but plasma membrane damage is prominent (Straub et al., 1997). Collectively, these findings suggest that ECM

receptors of the integrin family and their effectors control MTJ stability, whereas the DGC has a major function in maintaining the integrity of the sarcolemma.

We thank Ulrike Mayer (University of East Anglia) and Cary Wu (University of Pittsburgh) for generously providing us with antibodies to the integrin α7-subunit and Ilk, respectively. We thank Dusko Trajkovic for help with histology. This research was funded with support from the National Institute of Health to U.M. (NS046456) and R.L. (AR40050) and from the Wellcome Trust to D.R.C. (O77532).

Supplementary material

Supplementary material for this article is available at http://dev.biologists.org/cgi/content/full/135/11/2043/DC1

References

Armstrong, R. B., Ogilvie, R. W. and Schwane, J. A. (1983). Eccentric exercise-induced injury to rat skeletal muscle. *J. Appl. Physiol.* **54**, 80-93.

Balaban, N. Q., Schwarz, U. S., Riveline, D., Goichberg, P., Tzur, G., Sabanay, I., Mahalu, D., Safran, S., Bershadsky, A., Addadi, L. et al. (2001). Force and focal adhesion assembly: a close relationship studied using elastic micropatterned substrates. *Nat. Cell Biol.* **3**, 466-472.

Borowsky, M. L. and Hynes, R. O. (1998). Layilin, a novel talin-binding transmembrane protein homologous with C-type lectins, is localized in membrane ruffles. *J. Cell Biol.* **143**, 429-442.

Brabant, M. C., Fristrom, D., Bunch, T. A. and Brower, D. L. (1996). Distinct spatial and temporal functions for PS integrins during Drosophila wing morphogenesis. *Development* **122**, 3307-3317.

Brown, N. H. (1994). Null mutations in the alpha PS2 and beta PS integrin subunit genes have distinct phenotypes. *Development* **120**, 1221-1231.

Brown, N. H., Gregory, S. L., Rickoll, W. L., Fessler, L. I., Prout, M., White, R. A. and Fristrom, J. W. (2002). Talin is essential for integrin function in Drosophila. *Dev. Cell* **3**, 569-579.

Calderwood, D. A. (2004a). Integrin activation. *J. Cell Sci.* **117**, 657-666.

Calderwood, D. A. (2004b). Talin controls integrin activation. *Biochem. Soc. Trans.* **32**, 434-437.

Campbell, I. D. and Ginsberg, M. H. (2004). The talin-tail interaction places integrin activation on FERM ground. *Trends Biochem. Sci.* **29**, 429-435.

Carpenter, S. and Karpati, G. (1979). Duchenne muscular dystrophy: plasma membrane loss initiates muscle cell necrosis unless it is repaired. *Brain* **102**, 147-161.

Chen, H. C., Appeddu, P. A., Parsons, J. T., Hildebrand, J. D., Schaller, M. D. and Guan, J. L. (1995). Interaction of focal adhesion kinase with cytoskeletal protein talin. *J. Biol. Chem.* **270**, 16995-16999.

Choquet, D., Felsenfeld, D. P. and Sheetz, M. P. (1997). Extracellular matrix rigidity causes strengthening of integrin-cytoskeleton linkages. *Cell* **88**, 39-48.

Cram, E. J., Clark, S. G. and Schwarzbauer, J. E. (2003). Talin loss-of-function uncovers roles in cell contractility and migration in C. elegans. *J. Cell Sci.* **116**, 3871-3878.

Critchley, D. R. (2000). Focal adhesions – the cytoskeletal connection. *Curr. Opin. Cell Biol.* **12**, 133-139.

Davies, K. E. and Nowak, K. J. (2006). Molecular mechanisms of muscular dystrophies: old and new players. *Nat. Rev. Mol. Cell Biol.* **7**, 762-773.

Durbeej, M. and Campbell, K. P. (2002). Muscular dystrophies involving the dystrophin-glycoprotein complex: an overview of current mouse models. *Curr. Opin. Genet. Dev.* **12**, 349-361.

Durbeej, M., Henry, M. D. and Campbell, K. P. (1998). Dystroglycan in development and disease. *Curr. Opin. Cell Biol.* **10**, 594-601.

Frenette, J. and Tidball, J. G. (1998). Mechanical loading regulates expression of talin and its mRNA, which are concentrated at myotendinous junctions. *Am. J. Physiol.* **275**, C818-C825.

Galbraith, C. G., Yamada, K. M. and Sheetz, M. P. (2002). The relationship between force and focal complex development. *J. Cell Biol.* **159**, 695-705.

Geiger, B., Bershadsky, A., Pankov, R. and Yamada, K. M. (2001). Transmembrane crosstalk between the extracellular matrix-cytoskeleton crosstalk. *Nat. Rev. Mol. Cell Biol.* **2**, 793-805.

Gettner, S. N., Kenyon, C. and Reichardt, L. F. (1995). Characterization of beta pat-3 heterodimers, a family of essential integrin receptors in C. elegans. *J. Cell Biol.* **129**, 1127-1141.

Giannone, G., Jiang, G., Sutton, D. H., Critchley, D. R. and Sheetz, M. P. (2003). Talin1 is critical for force-dependent reinforcement of initial integrin-cytoskeleton bonds but not tyrosine kinase activation. *J. Cell Biol.* **163**, 409-419.

Ginsberg, M. H., Partridge, A. and Shattil, S. J. (2005). Integrin regulation. *Curr. Opin. Cell Biol.* **17**, 509-516.

Gullberg, D., Velling, T., Lohikangas, L. and Tiger, C. F. (1998). Integrins during muscle development and in muscular dystrophies. *Front. Biosci.* **3**, D1039-D1050.

Hamer, P. W., McGeachie, J. M., Davies, M. J. and Grounds, M. D. (2002). Evans Blue Dye as an in vivo marker of myofibre damage: optimising parameters for detecting initial myofibre membrane permeability. *J. Anat.* **200**, 69-79.

Hayashi, Y. K., Chou, F. L., Engvall, E., Ogawa, M., Matsuda, C., Hirabayashi, S., Yokochi, K., Ziober, B. L., Kramer, R. H., Kaufman, S. J. et al. (1998). Mutations in the integrin alpha7 gene cause congenital myopathy. *Nat. Genet.* **19**, 94-97.

Hynes, R. O. (1992). Integrins: versatility, modulation, and signaling in cell adhesion. *Cell* **69**, 11-25.

Jiang, G., Giannone, G., Critchley, D. R., Fukumoto, E. and Sheetz, M. P. (2003). Two-piconewton slip bond between fibronectin and the cytoskeleton depends on talin. *Nature* **424**, 334-337.

Lee, M., Cram, E. J., Shen, B. and Schwarzbauer, J. E. (2001). Roles for beta(pat-3) integrins in development and function of Caenorhabditis elegans muscles and gonads. *J. Biol. Chem.* **276**, 36404-36410.

Leptin, M., Bogaert, T., Lehmann, R. and Wilcox, M. (1989). The function of PS integrins during Drosophila embryogenesis. *Cell* **56**, 401-408.

Leu, M., Bellmunt, E., Schwander, M., Farinas, I., Brenner, H. R. and Muller, U. (2003). Erbb2 regulates neuromuscular synapse formation and is essential for muscle spindle development. *Development* **130**, 2291-2301.

Li, F., Zhang, Y. and Wu, C. (1999). Integrin-linked kinase is localized to cell-matrix focal adhesions but not cell-cell adhesion sites and the focal adhesion localization of integrin-linked kinase is regulated by the PINCH-binding ANK repeats. *J. Cell Sci.* **112**, 4589-4599.

Lieber, R. L., Woodburn, T. M. and Friden, J. (1991). Muscle damage induced by eccentric contractions of 25% strain. *J. Appl. Physiol.* **70**, 2498-2507.

Liu, S., Calderwood, D. A. and Ginsberg, M. H. (2000). Integrin cytoplasmic domain-binding proteins. *J. Cell Sci.* **113**, 3563-3571.

Livak, K. J. and Schmittgen, T. D. (2001). Analysis of relative gene expression data using real-time quantitative PCR and the 2(-Delta Delta C(T)) method. *Methods* **25**, 402-408.

Mayer, U., Saher, G., Fassler, R., Bornemann, A., Echtermeyer, F., von der Mark, H., Miosge, N., Poschl, E. and von der Mark, K. (1997). Absence of integrin alpha 7 causes a novel form of muscular dystrophy. *Nat. Genet.* **17**, 318-323.

McCann, R. O. and Craig, S. W. (1997). The I/LWEQ module: a conserved sequence that signifies F-actin binding in functionally diverse proteins from yeast to mammals. *Proc. Natl. Acad. Sci. USA* **94**, 5679-5684.

McCann, R. O. and Craig, S. W. (1999). Functional genomic analysis reveals the utility of the I/LWEQ module as a predictor of protein:actin interaction. *Biochem. Biophys. Res. Commun.* **266**, 135-140.

McNeil, P. L. and Khakee, R. (1992). Disruptions of muscle fiber plasma membranes. Role in exercise-induced damage. *Am. J. Pathol.* **140**, 1097-1109.

Miosge, N., Klenczar, C., Herken, R., Willem, M. and Mayer, U. (1999). Organization of the myotendinous junction is dependent on the presence of alpha7beta1 integrin. *Lab. Invest.* **79**, 1591-1599.

Mitra, S. K., Hanson, D. A. and Schlaepfer, D. D. (2005). Focal adhesion kinase: in command and control of cell motility. *Nat. Rev. Mol. Cell Biol.* **6**, 56-68.

Monkley, S. J., Zhou, X. H., Kinston, S. J., Giblett, S. M., Hemmings, L., Priddle, H., Brown, J. E., Pritchard, C. A., Critchley, D. R. and Fassler, R. (2000). Disruption of the talin gene arrests mouse development at the gastrulation stage. *Dev. Dyn.* **219**, 560-574.

Monkley, S. J., Pritchard, C. A. and Critchley, D. R. (2001). Analysis of the mammalian talin2 gene TLN2. *Biochem. Biophys. Res. Commun.* **286**, 880-885.

Nieswandt, B., Moser, M., Pleines, I., Varga-Szabo, D., Monkley, S., Critchley, D. and Fassler, R. (2007). Loss of talin1 in platelets abrogates integrin activation, platelet aggregation, and thrombus formation in vitro and in vivo. *J. Exp. Med.* **204**, 3113-3118.

Petrich, B. G., Marchese, P., Ruggeri, Z. M., Spiess, S., Weichert, R. A., Ye, F., Tiedt, R., Skoda, R. C., Monkley, S. J., Critchley, D. R. et al. (2007). Talin is required for integrin-mediated platelet function in hemostasis and thrombosis. *J. Exp. Med.* **204**, 3103-3111.

Riveline, D., Zamir, E., Balaban, N. Q., Schwarz, U. S., Ishizaki, T., Narumiya, S., Kam, Z., Geiger, B. and Bershadsky, A. D. (2001). Focal contacts as mechanosensors: externally applied local mechanical force induces growth of focal contacts by an mDia1-dependent and ROCK-independent mechanism. *J. Cell Biol.* **153**, 1175-1186.

Rooney, J. E., Welser, J. V., Dechert, M. A., Flintoff-Dye, N. L., Kaufman, S. J. and Burkin, D. J. (2006). Severe muscular dystrophy in mice that lack dystrophin and alpha7 integrin. *J. Cell Sci.* **119**, 2185-2195.

Rosalki, S. B. (1989). Serum enzymes in disease of skeletal muscle. *Clin. Lab. Med.* **9**, 767-781.

Sam, M., Shah, S., Friden, J., Milner, D. J., Capetanaki, Y. and Lieber, R. L. (2000). Desmin knockout muscles generate lower stress and are less vulnerable to injury compared with wild-type muscles. *Am. J. Physiol. Cell Physiol.* **279**, C1116-C1122.

Schmalbruch, H. (1975). Segmental fibre breakdown and defects of the plasmalemma in diseased human muscles. *Acta Neuropathol.* **33**, 129-141.

Schwander, M., Leu, M., Stumm, M., Dorchies, O. M., Ruegg, U. T., Schittny, J. and Muller, U. (2003). Beta1 integrins regulate myoblast fusion and sarcomere assembly. *Dev. Cell* **4**, 673-685.
Schwenk, F., Baron, U. and Rajewsky, K. (1995). A cre-transgenic mouse strain for the ubiquitous deletion of loxP-flanked gene segments including deletion in germ cells. *Nucleic Acids Res.* **23**, 5080-5081.
Senetar, M. A. and McCann, R. O. (2005). Gene duplication and functional divergence during evolution of the cytoskeletal linker protein talin. *Gene* **362**, 141-152.
Senetar, M. A., Foster, S. J. and McCann, R. O. (2004). Intrasteric inhibition mediates the interaction of the I/LWEQ module proteins Talin1, Talin2, Hip1, and Hip12 with actin. *Biochemistry* **43**, 15418-15428.
Senetar, M. A., Moncman, C. L. and McCann, R. O. (2007). Talin2 is induced during striated muscle differentiation and is targeted to stable adhesion complexes in mature muscle. *Cell Motil. Cytoskeleton* **64**, 157-173.
Shi, X. and Garry, D. J. (2006). Muscle stem cells in development, regeneration, and disease. *Genes Dev.* **20**, 1692-1708.
Sonnemann, K. J., Fitzsimons, D. P., Patel, J. R., Liu, Y., Schneider, M. F., Moss, R. L. and Ervasti, J. M. (2006). Cytoplasmic gamma-actin is not required for skeletal muscle development but its absence leads to a progressive myopathy. *Dev. Cell* **11**, 387-397.
Straub, V., Rafael, J. A., Chamberlain, J. S. and Campbell, K. P. (1997). Animal models for muscular dystrophy show different patterns of sarcolemmal disruption. *J. Cell Biol.* **139**, 375-385.
Taverna, D., Disatnik, M. H., Rayburn, H., Bronson, R. T., Yang, J., Rando, T. A. and Hynes, R. O. (1998). Dystrophic muscle in mice chimeric for expression of alpha5 integrin. *J. Cell Biol.* **143**, 849-859.
Tidball, J. G., O'Halloran, T. and Burridge, K. (1986). Talin at myotendinous junctions. *J. Cell Biol.* **103**, 1465-1472.
Vilquin, J. T., Brussee, V., Asselin, I., Kinoshita, I., Gingras, M. and Tremblay, J. P. (1998). Evidence of mdx mouse skeletal muscle fragility in vivo by eccentric running exercise. *Muscle Nerve* **21**, 567-576.
Volk, T., Fessler, L. I. and Fessler, J. H. (1990). A role for integrin in the formation of sarcomeric cytoarchitecture. *Cell* **63**, 525-536.
Weller, B., Karpati, G. and Carpenter, S. (1990). Dystrophin-deficient mdx muscle fibers are preferentially vulnerable to necrosis induced by experimental lengthening contractions. *J. Neurol. Sci.* **100**, 9-13.
Ziegler, W. H., Liddington, R. C. and Critchley, D. R. (2006). The structure and regulation of vinculin. *Trends Cell Biol.* **16**, 453-460.